Nanoaperture-Enhanced Signal-to-Noise Ratio in Fluorescence Correlation Spectroscopy

ARTICLE *in* ANALYTICAL CHEMISTRY · JANUARY 2009

Impact Factor: 5.64 · DOI: 10.1021/ac8024015 · Source: PubMed

4 AUTHORS, INCLUDING:

Jerome Wenger
French National Centre for Scientific Resea…
191 PUBLICATIONS **2,775** CITATIONS
SEE PROFILE

Davy Gérard
Université de Technologie de Troyes
72 PUBLICATIONS **860** CITATIONS
SEE PROFILE

Anal. Chem. **2008,** *80,* 6800–6804

Disposable Microscope Objective Lenses for Fluorescence Correlation Spectroscopy Using Latex Microspheres

Jérôme Wenger,* Davy Gérard, Heykel Aouani, and Hervé Rigneault

Institut Fresnel, Aix-Marseille Université, CNRS, 13397 Marseille, France

We explore the combination of a latex microsphere with a low NA lens to form a high performance optical system, and enable the detection of single molecules by fluorescence correlation spectroscopy (FCS). Viable FCS experiments at concentrations 1−1000 nM with different objectives costing less than $40 are demonstrated. This offers a simple and low-cost alternative to the conventional complex microscope objectives.

Fluorescence correlation spectroscopy (FCS) is widely recognized to be a powerful and versatile tool for the detection of a low amount of biomolecules.[1] By investigating the temporal dynamics of the fluorescence intensity, FCS can determine a wide range of molecular parameters, including molecular concentrations, translational and rotational diffusion coefficients, chemical rate constants, and binding rates.[2–4]

A critical issue in FCS is to discriminate the fluctuating signal from the noise, which requires simultaneously high fluorescence count rates per molecule (CRM) and low background.[5] Therefore, FCS is commonly implemented on a confocal microscope with a high-end immersion objective, providing high resolution and large numerical aperture (NA). Despite its extreme sensitivity (down to the single molecule), this approach remains expensive and difficult to integrate onto a laboratory-on-a-chip format.

A large part of the complexity and the cost of conventional FCS setups is related to the high NA microscope objective. Replacing this complex optical element by a simpler system would greatly extend the use of FCS for analytical biochemistry on chip. However, swapping the microscope objective to a single lens is not that easy. Any attempt to use low-cost objective lenses with reduced NA will face two major problems. First, the confocal observation volume V_{eff} will be enlarged, as V_{eff} scales with $1/\text{NA}^4$. This leads to a lower excitation intensity and CRM, a larger influence of the background noise due to Rayleigh and Raman scattering from the buffer solution, an increased effect of photobleaching due to the longer transit time of the molecules through the illuminated region, and a smaller range of molecular concentrations for FCS. Second, the count rate per molecule CRM dramatically decreases as NA is lowered, due to a lower excitation intensity and collection efficiency. For instance, substituting a 0.4 NA lens to a 1.2 NA water immersion objective leads to a 60× CRM decrease and V_{eff} increase, which makes any FCS experiment very difficult. In the context of designing low-cost laboratory-on-a-chip systems for analytical biochemistry, innovative alternatives to the high NA microscope objective have thus to be proposed.

Much attention has been recently devoted to the use of novel nanophotonics techniques to improve FCS with single molecule resolution at high concentrations (see ref 3 for a review). These techniques include total internal reflection illumination,[6] supercritical angle collection,[7,8] stimulated emission depletion,[9] near-field scanning microscopy,[10] microfluidic channels [11,12] or nanometric apertures.[13,14] If they perform well in a laboratory environment, all the aforementioned techniques rely on expensive and complex instrumentations. Therefore, they are not designed for an integration into a low-cost laboratory-on-a-chip device.

Looking for simpler and more cost-efficient systems, the use of a single-element aspheric lens for FCS has been investigated in ref 15. The specifically designed aspheric lens has 0.9 NA, which allows for efficiently detecting the fluorescence of a single molecule. Because of spherical and chromatic aberrations, the observation volume remained large $V_{\text{eff}} \approx 110$ fL, which limited the concentration range for FCS to 0.01−10 nM. To perform FCS at higher molecular concentrations without the need for a high NA microscope objective, an option is to combine a 0.6 NA air objective to a solid immersion lens (SIL).[16] A SIL is a hemisphere

(1) Eigen, M.; Rigler, R. *Proc. Natl. Acad. Sci. U.S.A.* **1994**, *91*, 5740–5747.
(2) Rigler, R.; Elson, E. S. *Fluorescence correlation spectroscopy, Theory and Applications*; Springer: Berlin, 2001.
(3) Blom, H.; Kastrup, L.; Eggeling, C. *Curr. Pharm. Biotechnol.* **2006**, *7*, 51–66.
(4) Briddon, S. J.; Hill, S. J. *Trends Pharmacol. Sci.* **2007**, *28*, 637–645.
(5) Zander, C.; Enderlein J.; Keller, R. A. *Single-Molecule Detection in Solution—Methods and Applications*; VCH-Wiley: Berlin/New York, 2002.
(6) Hassler, K.; Leutenegger, M.; Rigler, P.; Rao, R.; Rigler, R.; Gösch, M.; Lasser, T. *Opt. Express* **2005**, *13*, 7415–7423.
(7) Ruckstuhl, T.; Enderlein, J.; Jung, S.; Seeger, S. *Anal. Chem.* **2000**, *72*, 2117–2123.
(8) Ries, J.; Ruckstuhl, T.; Verdes, D.; Schwille, P. *Biophys. J.* **2008**, *94*, 221–229.
(9) Kastrup, L.; Blom, H.; Eggeling, C.; Hell, S. W. *Phys. Rev. Lett.* **2005**, *94*, 178104.
(10) Lewis, A.; Taha, H.; Strinkovski, A.; Menevitch, A.; Katchatouriants, A.; Dekhter, R.; Amman, E. *Nat. Biotechnol.* **2003**, *21*, 1378–1386.
(11) Foquet, M.; Korlach, J.; Zipfel, W. R.; Webb, W. W.; Craighead, H. G. *Anal. Chem.* **2004**, *76*, 1618–1626.
(12) Yin, D.; Lunt, E. J.; Barman, A.; Hawkins, A. R.; Schmidt, H. *Opt. Express* **2007**, *15*, 7290–7295.
(13) Levene, M. J.; Korlach, J.; Turner, S. W.; Foquet, M.; Craighead, H. G.; Webb, W. W. *Science* **2003**, *299*, 682–686.
(14) Rigneault, H.; Capoulade, J.; Dintinger, J.; Wenger, J.; Bonod, N.; Popov, E.; Ebbesen, T. W.; Lenne, P.-F. *Phys. Rev. Lett.* **2005**, *95*, 117401.
(15) Sonehara, T.; Anazawa, T.; Uchida, K. *Anal. Chem.* **2006**, *78*, 8395–8405.
(16) Serov, A.; Rao, R.; Gösch, M.; Anhut, T.; Martin, D.; Brunner, R.; Rigler, R.; Lasser, T. *Biosens. Bioelectron.* **2004**, *20*, 431–435.

10.1021/ac801016z CCC: $40.75
Published on Web 08/06/2008

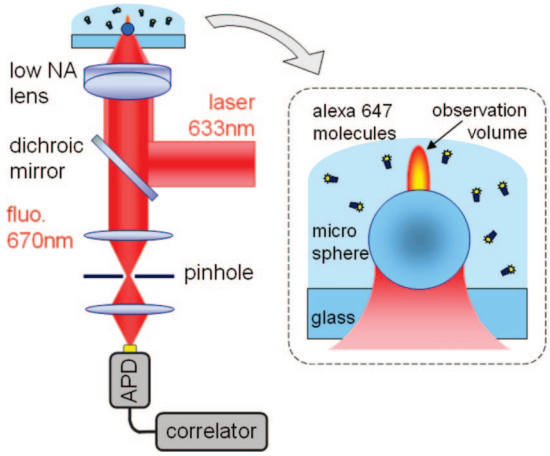

Figure 1. Schematics of the experimental setup (APD: avalanche photodiode).

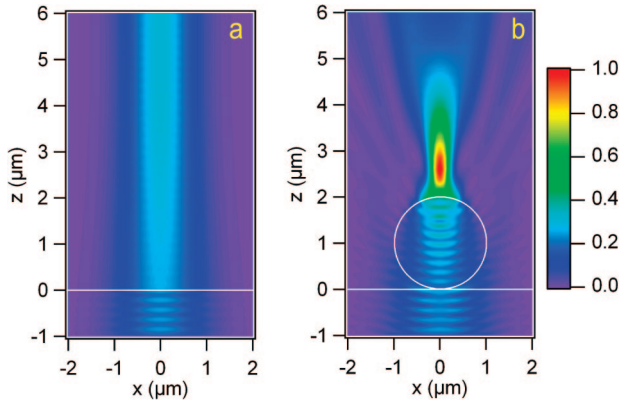

Figure 2. FDTD-calculated electric field intensity without (a) and with (b) a 2 μm cylinder illuminated by a Gaussian beam at $\lambda = 633$ nm with NA = 0.3.

made in a material of high refractive index that is set at the focus of a microscope objective to further increase the overall NA of the whole system.[17,18] Experiments performed on a commercial FCS apparatus (Zeiss ConfoCorr 1) have shown 50% higher collection efficiency and better field confinement for the SIL system in comparison to the conventional confocal setup. However, this kind of system is still far from a low-cost objective for integrated FCS.

In this study, we keep the working principle of SIL (that is to set a refractive device at the focus of a lens to increase its effective NA), but with a much simpler and cost-effective system: the SIL is replaced by a micron-sized latex sphere, and the microscope objective is formed by a simple lens (Figure 1). Thanks to the microsphere, the excitation beam is further focused and the fluorescence collection efficiency is improved. This configuration circumvents the drawbacks introduced by the use of the low-NA objective. Throughout this study, we use commercially available lenses, and look specifically for the simplest and cheapest way to replace the complex high-NA microscope objective. Below, we demonstrate viable FCS experiments at concentrations 1−1000 nM with different objectives costing less than $40.

(17) Koyama, K.; Yoshita, M.; Baba, M.; Suemoto, T.; Akiyama, H. *Appl. Phys. Lett.* **1999**, *75*, 1667–1669.
(18) Rao, R.; Mitic, J.; Serov, A.; Leitgeb, R. A.; Lasser, T. *Opt. Commun.* **2007**, *271*, 462–469.

Table 1. Specifications of the Different Objective Lenses Used in This Work[a]

designation	Thor4.6	Thor16	Zeiss10x	Zeiss40x
manufacturer	Thorlabs	Thorlabs	Carl Zeiss	Carl Zeiss
reference	CAY046	AC080-016-A1	Plan Neoflur	C-Apochromat
type	plastic	doublet	compound	compound
focal length	4.6 mm	16 mm	16 mm	4.0 mm
diameter	3.7 mm	8.0 mm	9.5 mm	9.5 mm
NA	0.4	0.25	0.3	1.2
magnification	35	10	10	40
indicative price	$4.20	$34.90	$350	$12,000

[a] The magnification is computed for a tube lens of 160 mm focal length.

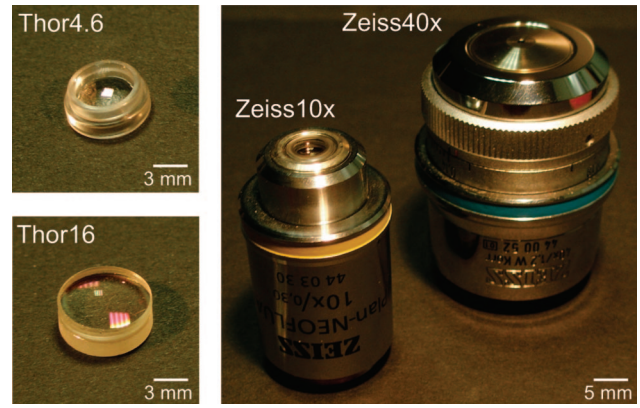

Figure 3. Photograph of the different objective lenses used in this work.

ELECTROMAGNETIC SIMULATIONS

Our results are strongly related to the electromagnetic field distribution in the vicinity of a dielectric microsphere. Under collimated illumination, several recent papers have theoretically predicted the existence of a beam termed "photonic nanojet" that emerges from the microsphere with high intensity, subwavelength transverse dimensions and low divergence.[19–22] Photonic nanojets, which have been experimentally characterized in ref 23, can enhance nanoparticle backscattering,[24] and two-photon fluorescence with floating microspheres.[25] Here, we describe the combination of a latex microsphere with a low NA lens to form a high performance disposable optical system.

To investigate the interaction between a focused Gaussian laser beam and a microsphere, we have performed 2D finite-difference time-domain (FDTD) computations (Figure 2). The computational domain is set to 8 × 7 μm^2, with perfectly matched layers as boundary conditions. The bead is modeled by a dielectric cylinder (refractive index $n = 1.6$, 2 μm diameter), on a glass substrate ($n = 1.5$) with water embedding medium ($n = 1.33$). A Gaussian beam is focused by a perfect lens with NA = 0.3, which gives a diffraction-limited waist of 1.0 μm (Figure 2(a)). When a microsphere is set at the lens focal plane, the incident beam is further

(19) Chen, Z.; Taflove, A.; Backman, V. *Opt. Express* **2004**, *12*, 1214–1220.
(20) Li, X.; Chen, Z.; Taflove, A.; Backman, V. *Opt. Express* **2005**, *13*, 526–533.
(21) Lecler, S.; Takakura, Y.; Meyrueis, P. *Opt. Lett.* **2005**, *30*, 2641–2643.
(22) Itagi, A. V.; Challener, W. A. J. *Opt. Soc. Am. A* **2005**, *22*, 2847–2858.
(23) Ferrand, P.; Wenger, J.; Pianta, M.; Rigneault, H.; Devilez, A.; Stout, B.; Bonod, N.; Popov, E. *Opt. Express* **2008**, *16*, 6930–6940.
(24) Heifetz, A.; Huang, K.; Sahakian, A. V.; Li, X.; Taflove, A.; Backman, V. *Appl. Phys. Lett.* **2006**, *89*, 221118.
(25) Lecler, S.; Haacke, S.; Lecong, N.; Crégut, O.; Rehspringer, J.-L.; Hirlimann, C. *Opt. Express* **2007**, *15*, 4935–4942.

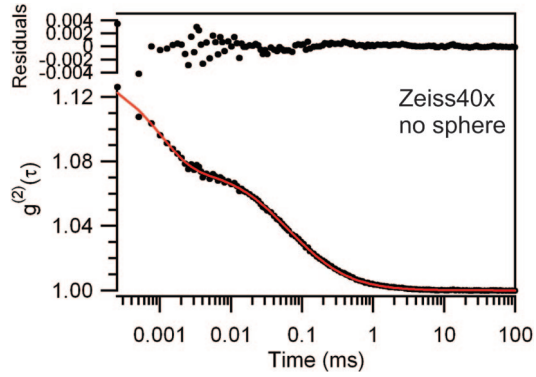

Figure 4. Reference correlation function (dots) recorded for Zeiss40x objective with no microsphere (dye concentration 40 nM, laser power $P_{laser} = 100\ \mu W$). Results from numerical fit (line) are summarized in Table 2.

focused (Figure 2(b)), in close fashion to photonic nanojets under plane wave illumination.[19,20] From Figure 2(b), we estimate the transverse and axial fwhm of 390 nm and 1.65 μm respectively, which come close to the values typically reached with a high NA objective. The extra focusing brought by the microsphere produces an enlarged effective numerical aperture, and further confines the observation volume. Reciprocally, the microsphere also allows for uncoupling the fluorescence light emitted at high angles.[7] Both effects contribute to the observations reported below of FCS using low-NA lenses and microspheres.

EXPERIMENTAL SECTION

Microspheres. Latex microspheres of well-calibrated diameter d_{sphere} (Fluka Chemie GmbH, diameter $d_{sphere} = 2$, 3, or 5 μm, refractive index 1.6, dispersion <0.1%) were diluted in pure water and dispersed on a cleaned microscope coverslip before air drying to ensure adhesion to the glass. The concentration was set to isolate one single bead per $10 \times 10\ \mu m^2$. When adding a solution of analytes, we observed that a reduced fraction of microspheres (about 10−20%) dissociated from the glass. The remaining fraction kept stuck to the substrate for the whole duration of the experiments.

Low NA Lenses. A set of different lenses was purchased directly from Thorlabs Inc. (Newton, NJ) with NA ranging from 0.2 to 0.4 and focal lengths from 4 to 25 mm. For the purpose of this study, we restrict to the lenses whose specifications are given in Table 1. The selection includes a plastic molded aspheric lens costing less than $5, and an achromatic spherical doublet of 16 mm focal length, which is broadly available at reduced costs (Figure 3). To go for higher optical complexity, we investigate the use of a classical 10×/NA 0.3/infinite correction microscope objective, which is probably the most common and widely used objective in microscopy laboratories. Last, to serve as a reference, we use Zeiss C-Apochromat 40×/NA 1.2/water immersion objective, which is specifically designed for confocal FCS.

FCS Setup. FCS experiments are conducted on a custom epifluorescence setup. Alexa-Fluor 647 dyes (A647) diluted in pure water to a concentration of 40 nM are excited by a focused He−Ne laser beam at 633 nm. The microsphere is positioned at the objective focus using a 3 axis piezoelectric stage (Polytek PI P527). The fluorescence is collected via the same objective, and filtered from the scattered laser light by a dichroic mirror (Omega Filters XF2072), followed by a long-pass filter (Omega Filters 640AELP). A 20 μm confocal pinhole conjugated to the microscope object plane rejects out-of-focus light. After the pinhole, the fluorescence is split by a 50/50 beamsplitter and focused on two avalanche photodiodes (Perkin-Elmer SPCM-AQR-13) with 670 ± 20 nm bandpass filters (Omega Filters 670DF40). The fluorescence intensity fluctuations $F(t)$ are analyzed by cross-correlating each photodiode signal with a hardware correlator (ALV-GmbH ALV6000) to compute the temporal correlation: $g^{(2)}(\tau) = \langle F(t) \cdot F(t + \tau) \rangle / \langle F(t) \rangle^2$, where $\langle\ \rangle$ stands for time-averaging. Each FCS measurement was obtained by averaging 20 runs of 10 s duration.

Table 2. Experimental Parameters and Results from the Numerical Fits of the FCS Data in Figures 4 and 5[a]

objective	Thor4.6	Thor16	Zeiss10x	Zeiss40x
d_{sphere} (μm)	2	3	2	
N	44	53.1	25.5	12.9
τ_d (μs)	54	62	68	62
s	0.17	0.15	0.20	0.25
n_T	0.8	0.9	0.9	0.8
τ_T (μs)	1.0	0.7	0.9	1.0
P_{laser} (mW)	0.5	0.2	0.2	0.1
CRM (kHz)	1.2	1.9	5.4	15.8
V_{eff} (fL)	1.7	2.0	1.0	0.5
C_{min} (nM)	0.5	0.4	0.8	1.7
C_{max} (μM)	1.0	0.8	1.6	3.4

[a] The observation volume V_{eff} is inferred from the number of molecules N given by FCS and the dye concentration (40 nM). The minimum and maximum concentrations C_{min} and C_{max} for FCS correspond to the concentrations for which the number of molecules N in the observation volume equals 0.5 and 1000 respectively.

FCS Data Analysis. We use the expression of the correlation function $g^{(2)}(\tau)$ for three-dimensional Brownian diffusion:[2,5]

$$g^{(2)}(\tau) = 1 + \frac{1}{N}\left(1 - \frac{B}{F}\right)^2\left[1 + n_T \exp\left(-\frac{\tau}{\tau_T}\right)\right] \times \frac{1}{(1 + \tau/\tau_d)\sqrt{1 + s^2\tau/\tau_d}} \quad (1)$$

where N is the total number of molecules, F the total signal, B the background noise, n_T the amplitude of the dark state population, τ_T the dark state blinking time, τ_d the mean diffusion time and s the ratio of transversal to axial dimensions of the analysis volume. Numerical fit of the FCS data following eq 1 provides the average number of molecules N, and therefore the fluorescence count rate per molecule CRM $= (F - B)/N$. The background noise B originates mainly from the back-reflected laser light and from the detector dark current. At 500 μW excitation power, it typically amounts to $B = 1.2$ kHz, which remains small as compared to the total fluorescence signal (given by $N \cdot$CRM).

RESULTS AND DISCUSSION

To keep a reference for conventional FCS with a high NA microscope objective, we plot the correlation function obtained for the objective Zeiss40x with no microsphere (Figure 4). Data obtained from numerical fits according to eq 1 are summarized in Table 2. With no surprise, the high 1.2 NA gives the lowest observation volume and the largest CRM. However, low NA lenses and microspheres can still perform decently, and for a fraction of the price.

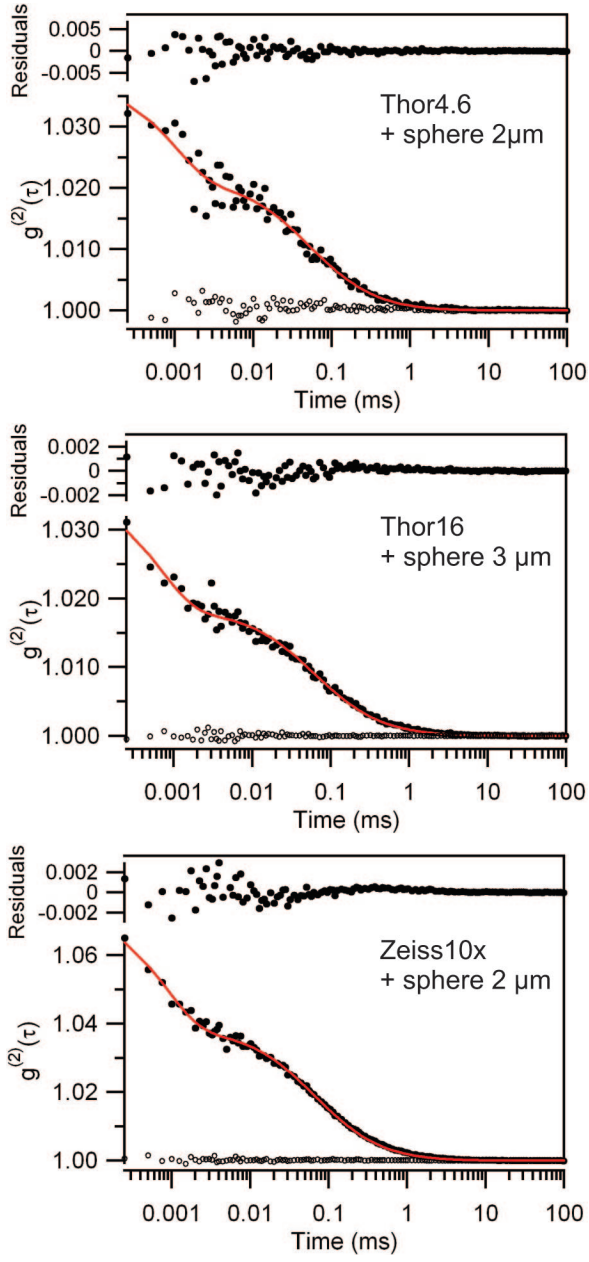

Figure 5. Correlation functions recorded for the different lenses specified in Table 1 with a single microsphere set at the lens focus. Empty markers show the correlation functions obtained without the microsphere. For all acquisitions, the dye concentration was kept at 40 nM. Results from numerical fits are detailed in Table 2.

Figure 5 presents typical correlation functions obtained with low NA lenses and microspheres instead of the Zeiss40x microscope objective. It clearly appears that usable correlation functions are readily obtained, despite the much lower numerical aperture of the lens. We stress that, without the latex sphere, no time correlation was found at all for the set of low NA lenses, resulting in flat correlation $g^{(2)}(\tau)$ functions. This originates from the combined effect of (i) reduced intensity fluctuations due to the large number of molecules in the observation volume, and (ii) the dramatically decreased CRM without the microsphere. When the microsphere is added, it compensates for these effects.

Experimental parameters and analysis of FCS data according to eq 1 are summarized in Table 2. The laser power P_{laser} corresponds to the incident power covering the back of the objective lens. We adjusted P_{laser} in order to obtain CRMs larger than 1 kHz. While increasing the excitation power, we experimentally checked that the fluorescence varied linearly with P_{laser} and that the number of molecules N stayed constant. Therefore, we ensure that we avoided the conditions leading to fluorescence saturation and photobleaching.

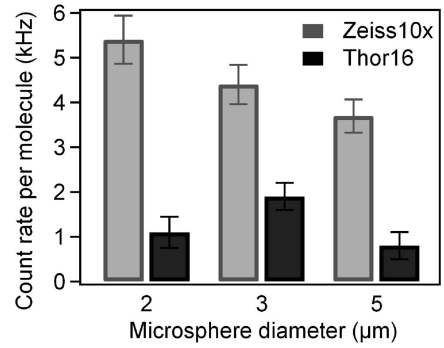

Figure 6. Average count rates per molecule for Zeiss10x and Thor16 lenses obtained for different microsphere diameters (the excitation power was kept at 200 μW for all these measurements). The error bars display the measurements' standard deviation.

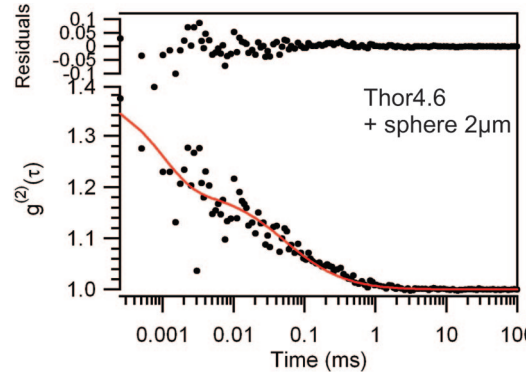

Figure 7. Correlation function showing the possibility to detect a single molecule with Thor4.6 objective and a 2 μm latex sphere (dye concentration 2 nM, laser power P_{laser} = 500 μW). Analysis based on eq 1 yields $N = 1.9$, $\tau_d = 58$ μs, and CRM = 1.0 kHz (due to the low signal-to-noise ratio, we fixed the following parameters: $n_T = 0.8$, $\tau_T = 1$ μs, $s = 0.17$).

Keeping the same dye concentration for all experimental runs allows a direct comparison between the number of detected molecules N and the effective observation volume V_{eff}. Depending on the overall optical magnification and the quality of the lens, the observation volume is enlarged by a factor 2−4 as compared to the standard Zeiss40x objective, but FCS is still possible in the range 1−1000 nM with CRMs higher than 1 kHz.

The optimal microsphere diameter leading to the best FCS data for each lens was found by direct experimentation. Figure 6 displays the CRMs found for Thor16 and Zeiss10x lenses with different microsphere diameters. A priori determining the optimal microsphere diameter is difficult because of the influence of spherical aberrations introduced by the low NA lens. This is evidenced by the comparison between the correlograms obtained for Thor16 and Zeiss10x lenses. Although both lenses bear similar optical specifications, the Zeiss10x objective performs much better in observation volume V_{eff} and CRM, as shown on Figure 6. We relate this effect to the influence of spherical aberrations that are only partly compensated for Thor16. Aberrations can dramatically

enlarge the spot diameter and lower the excitation intensity, but the microsphere partly compensates for these effects by selecting and focusing the fraction of the incident beam covered by the microsphere. For a perfect lens, we expect that the best particle diameter is close to the laser spot size, $d_{\text{sphere}} \approx \lambda/NA$. This condition ensures that all the excitation power can contribute to the photonic jet created by the sphere, and reciprocally, that the fluorescence emission collected by the sphere is best matched to the detection optics.[26] We point out that this condition is satisfied for the Zeiss10x objective, and not for the Thor16 lens. This latter discrepancy can again be understood as a consequence of spherical aberrations that enlarge the laser spot dimensions. Modeling the complete system formed by the microsphere and the low NA lens remains an open issue.

Positioning the microsphere with respect to the focus of the incident laser beam with 0.5 μm lateral and 2 μm resolutions was found sufficient. This is readily within the reach of standard translation stages. For laboratory-on-a-chip applications, we envision the permanent factory alignment of the microsphere respectively to the low NA lens to form a disposable optical system for single molecule detection.

Last, the dye concentration was diluted to 2 nM, to show the ability to detect single molecules with a $4 lens such as Thor4.6 assisted by a 2 μm latex sphere. Results are summarized in Figure 7. Due to a low signal-to-noise ratio (average fluorescence intensity 1.9 kHz, average background 1.3 kHz, signal-to-noise ratio ~1.5), the amplitude of the correlation function is lowered, but temporal correlations are still detectable. Numerical analysis yields an average number of molecules $N = 1.9$, which clearly illustrates the single molecule resolution of our system.

(26) Yi, K. J.; Wang, H.; Lu, Y. F.; Yang, Z. Y. J. *Appl. Phys.* **2007**, *101*, 063528.

CONCLUSION

In conclusion, we have demonstrated that a latex microsphere can be combined with a low NA lens to form a high-performance disposable optical system. This offers a simple and cheap alternative to the expensive and complex immersion objectives for FCS. Furthermore, the microsphere surface can be easily functionalized to enable simple and efficient monitoring of binding reactions. In the context of building laboratory-on-a-chip systems for high-throughput analytical biochemistry, we believe that dielectric microspheres can provide a low-cost and highly parallel means for studying single molecule dynamics at high concentrations.

ACKNOWLEDGMENT

The authors acknowledge stimulating discussions with E. Popov, N. Bonod, B. Stout, A. Devilez, D. Gachet and P. Ferrand. This work is funded by contract CNRS PEPS07 “NanoDrill”.

Received for review May 19, 2008. Accepted June 20, 2008.

AC801016Z